sustainability

MDPI

Review

Air Pollution and Its Association with the Greenland Ice Sheet Melt

Kumar Vikrant [1,†], Eilhann E. Kwon [2,†], Ki-Hyun Kim [1,*], Christian Sonne [3], Minsung Kang [4] and Zang-Ho Shon [4,*]

1 Department of Civil and Environmental Engineering, Hanyang University, Seoul 04763, Korea; vikrant23@hanyang.ac.kr
2 Department of Environment and Energy, Sejong University, Seoul 05005, Korea; ekwon74@sejong.ac.kr
3 Department of Bioscience, Aarhus University, DK-4000 Roskilde, Denmark; cs@bios.au.dk
4 Department of Environmental Engineering, Dong-Eui University, Busan 47340, Korea; pantome@naver.com
* Correspondence: kkim61@hanyang.ac.kr (K.-H.K.); zangho@deu.ac.kr (Z.-H.S.)
† Co-First author.

Abstract: The Greenland Ice Sheet (GrIS) has been a topic of extensive scientific research over the past several decades due to the exponential increase in its melting. The relationship between air pollution and GrIS melting was reviewed based on local emission of air pollutants, atmospheric circulation, natural and anthropogenic forcing, and ground/satellite-based measurements. Among multiple factors responsible for accelerated ice melting, greenhouse gases have long been thought to be the main reason. However, it is suggested that air pollution is another piece of the puzzle for this phenomenon. In particular, black carbon (BC) and other aerosols emitted anthropogenically interact with clouds and ice in the Arctic hemisphere to shorten the cloud lifespan and to change the surface albedo through alteration of the radiative balance. The presence of pollution plumes lowers the extent of super cooling required for cloud freezing by about 4 °C, while shortening the lifespan of clouds (e.g., by altering their free-energy barrier to prompt precipitation). Since the low-level clouds in the Arctic are 2–8 times more sensitive to air pollution (in terms of the radiative/microphysical properties) than other regions in the world, the melting of the GrIS can be stimulated by the reduction in cloud stability induced by air pollution. In this study, we reviewed the possible impact of air pollution on the melting of the GrIS in relation to meteorological processes and emission of light-absorbing impurities. Long-term variation of ground-based AERONET aerosol optical depth in Greenland supports the potential significance of local emission and long-range transport of air pollutants from Arctic circle and continents in the northern hemisphere in rapid GrIS melting trend.

Keywords: climate change; Greenland ice melt; meteorology; air pollution; cloud stability

Citation: Vikrant, K.; Kwon, E.E.; Kim, K.; Sonne, C.; Kang, M.; Shon, Z. Air Pollution and Its Association with the Greenland Ice Sheet Melt. *Sustainability* **2021**, *13*, 65. https://dx.doi.org/10.3390/su13010065

Received: 8 November 2020
Accepted: 21 December 2020
Published: 23 December 2020

1. Introduction

The Greenland Ice Sheet (GrIS) is about the same size as the state of Alaska in the USA and can result in the rise of the global sea level by more than 7.2 m upon complete melting [1]. It has been suggested that 70% of the 269 billion tons of ice lost from the GrIS during 2011–2014 has primarily been due to surface melts rather than the calving-based processes [2]. Although global warming induced by greenhouse gases has long been perceived as the major driver of this ice melt, the possible involvement of other factors and processes has been continuously questioned [3]. For instance, the role of air pollution (e.g., in the form of particulate matter released from the combustion of fossil fuels) is now proposed as one of the potential driving components in addition to all of those identified to date [4–6].

The occurrence of atmospheric Arctic currents/circulation such as the negative phase of the Arctic oscillation (AO) and north Atlantic oscillation (NAO) offers a measure for transporting or propagating the pollutants to or within remote areas even to places that

are remote from eminent man-made source processes (except volcanic activities) [7,8]. The evolution and transport of pollution plumes from the combustion of fossil fuels and biomass (particularly containing black carbon (BC)), if occurring, lowers the extent of super cooling required for cloud freezing by about 4 °C [7]. Figure 1 elucidates the super cooling freezing temperature (ΔT^*) based on the space observations for four different cloud types with four liquid-cloud-droplet effective radius (r_e) regimes. The ice fraction (χ_{Ice}) was calculated based on combined ice cloud-top and liquid temperature distributions [7]. In general, the average ΔT^* value was reduced by ~1 °C between the upper and lower regimes in r_e for all cloud types [7]. Such processes can shorten the lifespan of clouds by altering their free-energy barrier to prompt precipitation. Note that the error bars in Figure 1 represent the uncertainties calculated by Equation (1). It should be noted that a_2/a_1 is a parameter representing the super cooling temperature for which the ice-cloud fraction becomes equal to the liquid-cloud fraction as detailed in [7].

$$\delta(\Delta T)^2 = \Delta T^2 \left(\left(\frac{\delta a_2}{a_2} \right)^2 + \left(\frac{\delta a_1}{a_1} \right)^2 \right) \quad (1)$$

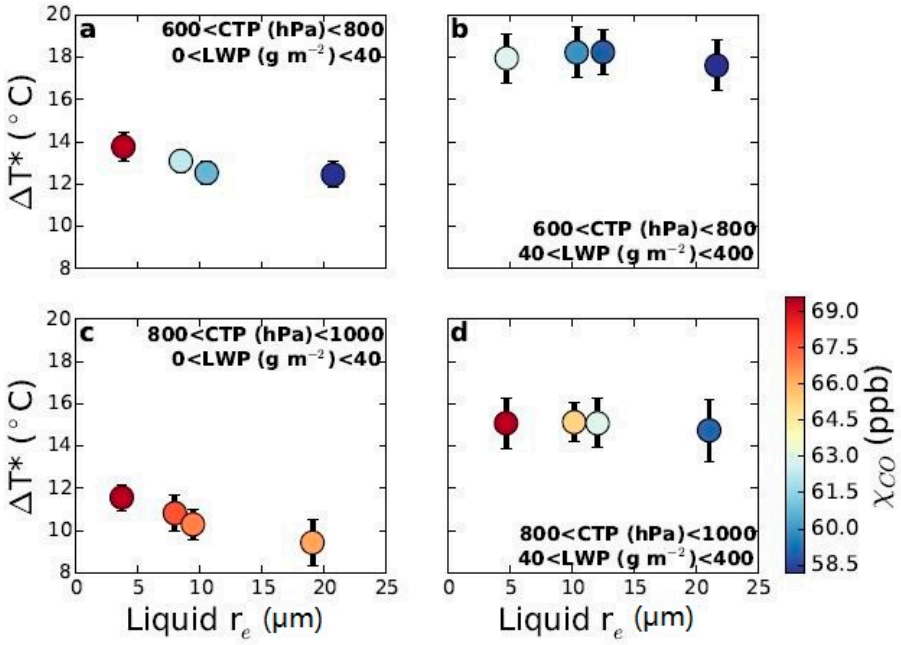

Figure 1. Super cooling freezing temperature (ΔT^*) versus the effective radius of the liquid-cloud-droplet (r_e) for four cloud category types (Panels (**a**–**d**)) differentiated by their top pressure (CTP) and liquid water path (LWP). The mean carbon monoxide (CO) concentration (χ_{CO}) is represented by the color scale; reproduced with permission from [7]. Detailed description of the utilized terms can be found in [7].

As can be seen in Figure 2, if no precipitation occurs during the transport of air pollutants to the Arctic region, then the net aerosol-cloud interaction parameter (ACI^{net}) value can be quantified based on the local efficiency of cloud property perturbation due to the increased aerosol quantities [5]. Under such a situation, the expected ACI^{net} values fell in the range of 0 to ~0.33 (theoretical maximum) [9]. In cases where precipitation occurs during the transport of pollutants to the Arctic region, aerosol particles may be scavenged via wet deposition only to leave carbon monoxide (CO) behind (utilized as a passive tracer). In such cases, the ACI^{net} value should remain zero even if the aerosols under consideration would have previously acted as effective cloud condensation nuclei (CCN) [10]. Thus, further research endeavors are needed to uncover the driving mechanisms and the resulting consequences of such air pollution-related side effects on the surface mass balance and ice

sheet albedo. In this regard, the present review article aims to catalyze scientific discussions towards such meteorological processes for better control of the Arctic ice melt crisis in this study.

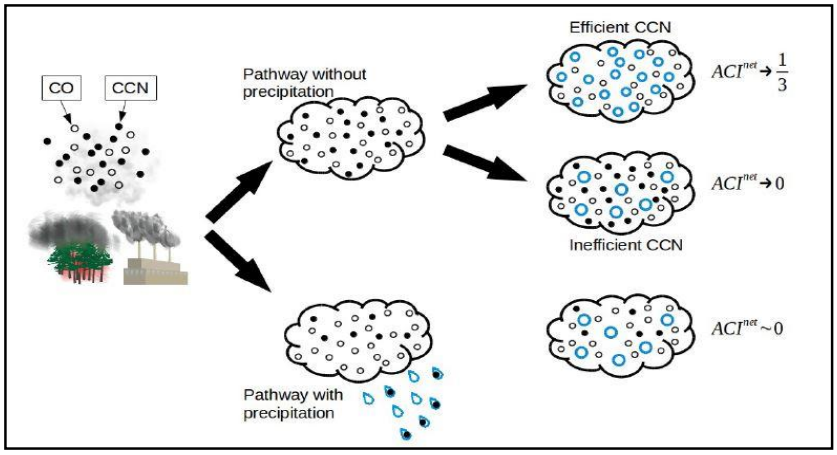

Figure 2. The relationship between aerosol concentrations (along various pathways for long-range transport) and a passive tracer (CO) in a tracer-based transport model. The correlation between aerosols and CO is established at the source region. Based on the occurrence of precipitation (during transport) and the aerosol efficiency to act as cloud condensation nuclei (CCN), the effect of pollution plumes (from distant regions) on clouds in the Arctic region specified by the net aerosol-cloud interaction parameter (ACI^{net}) varied between 0 and 1/3; reproduced with permission from [5].

2. Data Collection and Literature Survey Methodology

The dataset for the Greenland mass variation analysis (since 2002) was obtained from ice mass measurements by GRACE satellites (NASA) available from the website: https://climate.nasa.gov/vital-signs/ice-sheets/. A literature survey for the discussion of the relationship between air pollutants, such as BC/aerosol, and ice melting in the Arctic region was carried out using the Google Scholar search engine with key words of "ice melting", "BC", "ship", "biomass burning", "wildfire", and "absorption coefficient."

3. Radiation in the Arctic and Mass Loss of the GrIS

The radiative properties of mixed-phase clouds in the Arctic region play a crucial role in governing the ice sheet warming rate. Air pollutants can be transported into such remote areas due to the meteorological atmospheric currents/circulation patterns (e.g., negative phase of NAO) [7,8,11]. Thus, the reduction of cloud lifespans induced by air pollution may result in abnormal regulation of the Arctic surface temperature that can accelerate the ice-melting rate depending upon the season, sea-ice coverage, and cloud optical depth [5,7,12]. In addition, the presence of a warmer layer of air on top of colder air near the Arctic surface traps the particulate air pollutants for months and restricts their deposition onto the ice surface [13,14]. Furthermore, the stability of low-level clouds in the Arctic is 2–8 times more sensitive to air pollution (in terms of the radiative and microphysical properties) than in other regions of the world [5]. Such amplified sensitivity of clouds in the Arctic region may be accounted for by the diminished droplet evaporation rate due to an increase in the stability of lower troposphere and a decrease in the vertical cloud mixing possibility with the sub-saturated air [5]. As predicted through a numerical tracer transport model, the aerosol-cloud interactions over the Arctic Circle could efficiently exert pronounced negative impacts on the melting of GrIS due to air pollution, such as aerosols liberated from man-made consumption of fossil fuels relative to (natural) biomass burning [5,7,15]. A clear distinction as to why the stability of low-level clouds in the Arctic region is affected more detrimentally by aerosols derived from fossil fuel combustion than by those from biomass burning remains to be resolved via further research.

In recent years, GrIS has been losing about 280 Gt yr^{-1} on average [16,17]. According to data from NASA's GRACE and GRACE Follow-On satellites [18], the ice sheet in November 2019 had lost about 4700 Gt yr^{-1} of its mass since 2002 (e.g., rate of change in Greenland mass, −283 Gt yr^{-1}) due to an increase in the Arctic sea-surface temperature (e.g., Chukchi Sea: 0.07 ± 0.03 °C yr^{-1} for August of each year, 1982–2017, [16]). Furthermore, the recent rate of change in the Greenland mass (for 2010–2019) has slowed down by −218 Gt yr^{-1} (Figure 3).

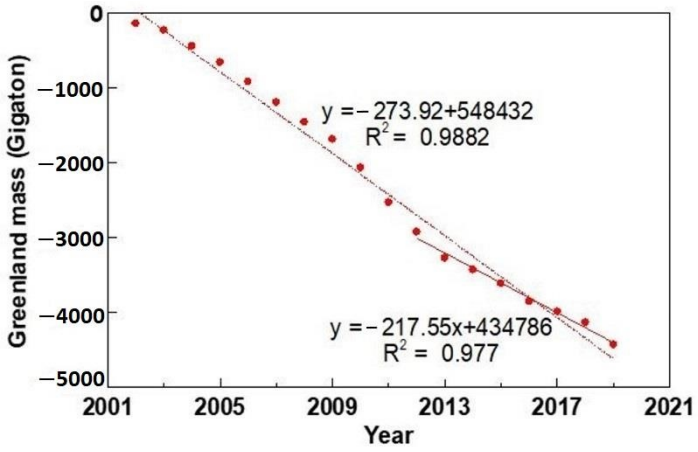

Figure 3. Variation of Greenland mass (in Gigatonne, [Gt]) since 2002 (Source of data: Ice mass measurement by GRACE satellites (NASA). Credit: NASA).

4. Atmospheric Circulation for the Transport of air Pollutants to GrIS

The most considerable mass loss in GrIS is from NW, SE, and CW regions of Greenland [19]. Anomalous GrIS melt episodes during the warm season often occur under slow-moving high-pressure regimes known as "Greenland blocks," with these blocking anticyclones favored during negative NAO conditions [20–23]. The NAO is a weather phenomenon in the North Atlantic Ocean of fluctuations in the sea level atmospheric pressure difference between the Icelandic Low and the Azores High. Through the fluctuations in the strength of the Icelandic low and the Azores high, it controls the strength and direction of westerly winds and location of storm tracks across the North Atlantic [24]. It is part of the Arctic oscillation that varies over time without particular periodicity. Negative NAO arises from Greenland blocking, while positive NAO mainly represents the absence of blocking [25]. Surface melt anomalies were concentrated across the western and southern GrIS during most of the high-melt seasons from the mid-2000s through the early 2010s because Greenland blocking, which is an essential contributor to recently enhanced GrIS melt rates, exerted a warming effect on West Greenland and Baffin Bay [26]. Greenland blocking has increased significantly in summer (June, July, and August (JJA)) over the past few decades [25,27].

Another form of synoptic atmospheric circulation feature that may exert an essential influence on GrIS surface mass balance (SMB) is the transport of water vapor by atmospheric rivers (ARs). Glacier SMB is the difference between accumulation and ablation (sublimation and melting) (e.g., negative SMB as retreat versus positive SMB as advance). As climate change may affect both temperature and snowfall in GrIS, changes in the SMB are to be accompanied. ARs are narrow corridors of strong horizontal water vapor transport through which most of the annual moisture transport into the high latitudes of the Northern Hemisphere are accomplished during a relatively small number of transient events [28–30]. GrIS mass loss arises directly from intense moisture transport over Greenland by ARs [31]. The occurrences of both extreme GrIS melting event (during July 2012) and the less extensive event (during early April 2016) should be ascribable to strong ARs. The strong ARs should have enhanced water vapor greenhouse effect, formation of clouds retaining additional longwave radiation, condensational latent heat release in the advected

air mass, and surface melt energy provided by liquid precipitation [32,33]. However, AR events can also provide positive inputs to SMB through snow accumulation. In addition, the AR events can decrease solar radiation over the low-albedo ablation zone [34]. Net AR impacts on SMB are likely to vary according to a number of factors such as season, elevation, latitude, and moisture transport intensity [35,36]. It was found that the observed overall trend in BC and sulfate measurement at the Arctic stations can be explained by the changes in their emissions while the long-term atmospheric circulation can only explain a minor fraction of the overall trend [37]. The positive correlation between NAO and concentrations of air pollutants was also found in Greenland ice cores [38] and Arctic stations [37]. Northern Eurasia is the region of dominant emission source for both BC and sulfate at all Arctic stations. There are indications that the BC emissions from Eurasia in wintertime have increased over the last decade, probably reflecting the emission increases in China and other East Asian countries [37]. Large-scale atmospheric circulation patterns such as negative NAO and Greenland blocking can transport air pollutants, which can enhance GrIS mass loss indirectly through absorbing solar radiation.

5. Air Pollution and Emissions

BC (and aerosol) in air has been reported to exert influences on climate change directly through radiative forcing and indirectly through cloud properties [16,39–45]. BC is typically produced from the incomplete combustion of natural biomass (wildfires) and fossil fuels (anthropogenic activities). Major emission sources of BC in the Arctic area are shipping and biomass burning (e.g., boreal wildfires) [46]. Wildfires in British Columbia and the northwest territories in 2017 were also reported to have contributed greatly to the enhancement of total column concentrations of trace gases, such as NH_3, CO, HCN, and C_2H_6, over a decadal-scale (1999–2017) based on ground-based observations [47]. This observation suggested the importance of wildfires as one of the driving forces affecting the Arctic climate.

Roughly two-thirds of the BC emissions (e.g., 193 tons) made in 2015 over the Arctic could be attributed to ships (e.g., general cargo, oil tankers, and fishing vessels) as the major consumers of heavy oil, which was largely by Russian vessels [48]. In the new millennium, there have been notable increases in Arctic ship traffic and associated BC emissions due to the long record of, on average, shipping of supplies for offshore gas/oil extraction industries, heightened last-chance tourism, and receding ice-sea extent [46,49]. BC emissions are projected to rise dramatically to 282 ton in 2025, which is an increase of 46% from 2015, if ships are diverted from the Suez and Panama canals to benefit from the shorter routes to the Arctic from Europe, Asia, and North America [48]. As such, the rising emissions of BC due to marine traffic in the Arctic could enhance Arctic warming primarily through decreases in the Arctic albedo [48,50,51].

Aerosols emitted from anthropogenic activities can interact with clouds in the Arctic Circle to potentially shorten their lifespan (as mentioned earlier in Section 1). The anthropogenic aerosol-cloud interaction can increase the droplet concentration, which, in turn, may heighten the cloud albedo [52]. Thus, the aerosol perturbations can impart evaporation-entrainment feedback (particularly for non-precipitating cumulus clouds) to shorten the cloud lifespan [52]. However, it was also reported that anthropogenic aerosols can suppress the precipitation to yield clouds with longer lifespans, higher liquid water content, and larger fractional cloudiness [52,53]. Hence, further studies are needed to clarify the contrasting observations to pinpoint the exact influence of anthropogenic aerosols on cloud lifespan in the Arctic region. The low-level clouds in the Arctic region are estimated to be 2–8 times more susceptible to air pollution than those in the rest of the world. This, in turn, could have severe adverse effects on the radiative balance in the Arctic region. Furthermore, as BC from wildfires has increased markedly in the atmosphere above the Arctic in a warmer climate [54], it can stimulate the deposition of BC on the GrIS to accelerate ice melting over time [55]. Wildfires can be held accountable for much of the documented inter-annual variability in the concentrations of carbonaceous aerosol that

induce changes in regional climate and air quality on an inter-annual cycle [56]. They have also been found to be major contributors to inducing an abnormal snowmelt rate in the arctic region [57]. However, long-term observations of BC made at three Arctic stations: Alert, Barrow, and Zeppelin, showed its downward trend (0.3–7.2%) of -2.1 ng m^{-3} yr^{-1} for 1998–2008, primarily due to the transport of air pollutants from Northern Eurasia and decreasing emissions [37,58]. A slower downward trend of -1.4 ng m^{-3} yr^{-1} was seen at Alert and Zeppelin for 2002–2009, while no such statistically significant trend was seen at Barrow. At Alert and Barrow, 2000–2001 saw a rise in BC concentrations [59]. The general downward trend (1989–2013) at Barrow, Alert, and Zeppelin was weakened after 2000 and a slight upward trend was seen at Barrow and Zeppelin after 2000 [40,60,61]. The overall decreasing trend in BC at those three stations was in contrast to the BC emission inventory estimated for the Svalbard area (including Zeppelin, 74° N–81° N, 10° E–35° E). It should be noted that strongly increasing emissions from 2000 to 2007 were mostly driven by increased shipping emissions [62].

The Global Fire Assimilation System (GFAS) can estimate the deposition of burning-derived BC on the GrIS. The daily estimates of BC emission from biomass burning and wildfires is facilitated by the satellite-based fire radiative power (FRP) observations of the GFAS [63–65]. The FRP is a quantitative measurement of the amount of energy released by burning and, hence, it is possible to project how much vegetation has been burned. It was found that the smoke plumes from wildfires were often pushed towards the GrIS by westerly winds [66]. Thus, a large fraction of the emissions (30%) was deposited on snow- or ice-covered surfaces. The calculated deposition was small compared to the deposition from global sources, although not entirely negligible. The albedo changes and instantaneous surface radiative forcing in Greenland due to the fire BC emissions were estimated to be relatively small (e.g., 0.006 for wildfires burned area (2345 ha) in western Greenland between 31 July and 21 August 2017) [66]. The large fraction of BC deposited on the GrIS made these fires very efficient climate forcers on a per unit emission basis. Substantial albedo changes and accelerated GrIS melting are expected to occur in the future as the warming of Greenland could produce wildfires at much larger scale. As limited satellite records are often obtainable for fires, the large inter-annual variability of fires around the globe limits our capacity to detect a change in the climate signal from the available global fire emission data [67–69].

A decline in the ice sheet albedo has been documented since the mid-1990s [17]. Because the surface melt in GrIS is closely connected to changes in the surface albedo, the assessment of multidecadal changes in the ice sheet albedo offers insight into surface melt and associated changes in its SMB. It was found that the rate of albedo decrease during summer melt has been accelerated during the 2000s (relative to the early 1980s). Furthermore, the surface albedos often decrease to values typical of bare ice at elevations 50–100 m above the ice sheet (analysis of the second edition of the satellite-derived climate data record (1982–2015) CLARA (The CM SAF cloud, Albedo and Surface Radiation dataset from Advanced Very High Resolution Radiometer (AVHRR) data-second edition denoted as CLARA-A2)) [70]. The southern margins exhibited the opposite behavior, probably due to increased snowfall over the area [70].

The albedo of snow (and sea ice) is affected by light-absorbing impurities and grain sizes, such as microbiota and BC [45,71–73]. The observed albedo decreases are closely tied to the increasing mass loss of the ice sheet by enhancing its surface melt [74,75]. The 1982–2015 decadal albedo trends reached a maximum of approximately -0.05 over the ablation region (dark zone area) in the Kangerlussuaq sector in July [70]. The albedo decreases along the west coast mainly occurred between 2000 and 2012 due to a change in atmospheric circulation, which promoted the advection of warm and moist southerly air masses along the west coast. Meanwhile, springtime darkening in Greenland since 2009 was attributed to a widespread increase in the amount of light-absorbing impurities in snow as well as in the atmosphere [76]. The enhancement BC concentrations was suggested to significantly contribute to albedo feedback that triggered the widespread 2012 melt [77].

The concentrations of BC and light-absorbing dust impurity were analyzed along with their impact on snow albedo during the 2012–2014 snowfall season across north-west Greenland [78]. Albedo reductions due to light-absorbing impurities are small with an average of 0.003 (episodic enhancements result in reductions in the 0.01–0.02 range). No significant increase in BC or dust concentrations was found relative to recent decades. Such an observation indicates that the enhanced deposition of light-absorbing impurities does not cause significant reduction in dry snow albedo or increases in melt events. Recently, the effect of pigmented glacier algae on albedo change was suggested as one of the causes for the surface darkening (both within and outside the south-west GrIS dark zone) [79].

In this study, the fine-mode aerosol optical depth (fAOD) and total AOD (Level 2.0, cloud-screened and quality-assured) data, derived from Sun photometer at ground-based Aerosol Robotic Network (AERONET) at four measurement sites during the summer season in Greenland, were analyzed to evaluate the long-term trend of column-integrated anthropogenic particulate pollutants. The fAOD is the product of the total AOD and the fine-mode fraction (FMF). AOD is a measure of the extinction of the solar beam by particles in the atmosphere (dust, smoke, and BC) relative to the aerosol amount in the vertical atmospheric column over the observation location. As shown in Figure 4, the upward trends of fAOD and AOD were observed at all sites in Greenland, except for a western site (Kangerlussuaq). In general, this positive correlation of fAOD with the melting of GrIS implies the significant role of anthropogenic air pollutants transported from Arctic regions in melting GrIS. Measurements of AOD in western Greenland were strongly influenced by forest fires in Canada and wildfires in Greenland [66]. In general, this positive correlation of fAOD with the melting of GrIS indicates the potent role of anthropogenic air pollutants transported from various Arctic regions. Thus, the discrepancy of the role of albedo change by light-absorbing impurities in GrIS melting should therefore be resolved in projections of Greenland mass loss.

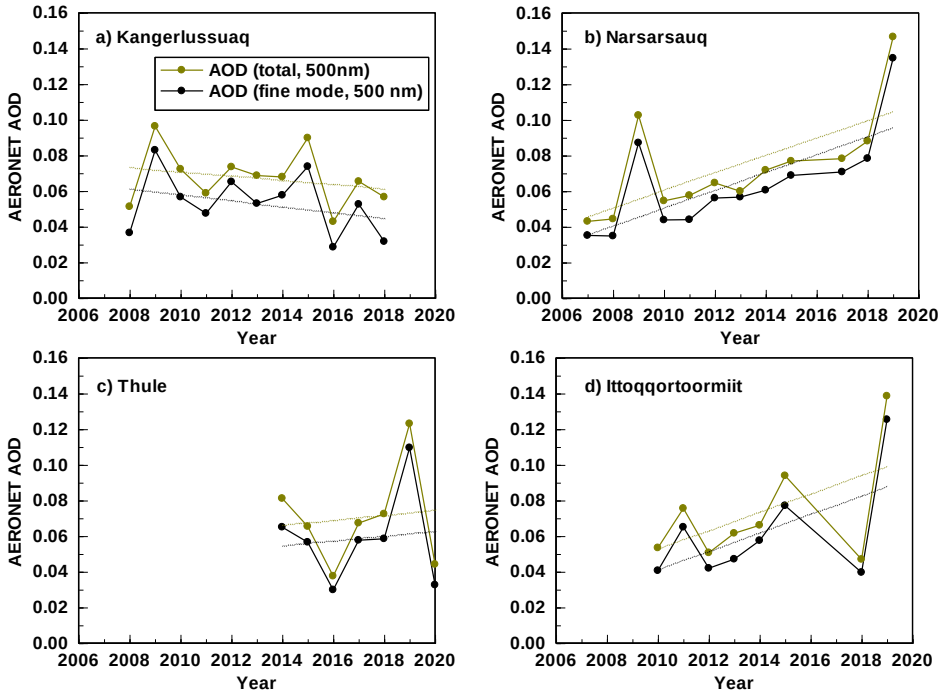

Figure 4. Yearly variation of AERONET total and fine-mode aerosol optical depths (AODs) at 500 nm during summer (June, July, and August (JJA)).

6. Light Absorption

The light absorbing fraction of carbonaceous aerosols in the Arctic air has also been measured in the form of an aerosol light absorption coefficient (AAC) by several light absorption methods (filter absorption photometry and photoacoustic photometry). Long-

term observations of BC optical properties were established after the discovery of Arctic haze, which includes a core monitoring site at Summit in Greenland (since 2003) [80,81]. The AACs in Svalbard showed a clear seasonality with the largest values being documented in the spring, and the smallest in the fall/summer seasons [82] due to the enhanced transportation of pollution from the mid-latitudes in the winter and spring [83], and the higher efficiency of wet removal in the summer [84]. In contrast to the direct measurement of GrIS melting with time, there are no generalized or clear trends for absorption and scattering coefficients for aerosol radiative properties for the past 10 years (2006–2018) in the Arctic region. Such limitations can be explained by the possibly large measurement uncertainties, which make it difficult to interpret the trend of evolving radiative properties in polar regions [85].

According to climate modeling, greenhouse gas warming of the Arctic climate should have been accelerated by global emissions of BC that absorbed solar energy in the atmosphere and snowpack [57,86–91]. In contrast, one climate-model study by [92] indicated the slight cooling of Arctic surface due to the presence of atmospheric BC in the Arctic region. Such a phenomenon was caused by the lowering of surface isolation and poleward energy flux. [44] found that the simulated distribution of Arctic atmospheric BC cooled the surface slightly, while the BC deposited by the local cryospheric atmosphere warmed the Arctic in line with the findings of [92]. Due to the model limitations in terms of indirect aerosol effect exclusion, ocean heat transport-mechanism changes, and radiative forcing, study of the Arctic climate response to BC is being explored further.

In addition to the deposition of BC on the GrIS, the role of actively photosynthesizing and heavily pigmented cyanobacteria and microalgae found on the bare ice is also important. These microbes darken the GrIS surface during the summer months to reduce albedo and speed up melting [71]. The potential of black-brown ice-algae and red/green snow algae in reducing ice and snow albedos was estimated to be high enough (between 30–40%) relative to clean ice and snow, respectively [71,73]. Thus, it is imperative to accurately assess the role of Arctic microbiota in the context of designing better climate change models and establishing proper preventive measures. The discussion on the role of such bacterial colonies in controlling the GrIS ice melting is not extended further, as it is beyond the scope of this review [93–95].

The Intergovernmental Panel on Climate Change (IPCC) announced on 25 September 2019, that a reduction in global air pollution is imperative to preserve the ecology of the cryosphere [3]. In addition, the "Ocean and Cryosphere in a Changing Climate" (IPCC special report) was accepted by 195 member governments to control the air pollutant emissions in accordance with the goals set in the 2015 Paris Agreement [3]. If the present usage of fossil fuels and associated resources to reduce aerosol emissions is not controlled properly, we may soon reach a tipping point [96,97] from which the meltdown of Greenland may proceed irreversibly with a catastrophic rise in sea-level over the next 1000 years. According to the same IPCC report, the tipping point may be reached even if anthropogenic CO_2 emissions are reduced to zero overnight due to other factors (e.g., afforestation/reforestation).

7. Conclusions

Review on relationship between air pollution and GrIS melting was reviewed based on local emission of air pollutants, atmospheric circulation, natural and anthropogenic forcing, and ground-based and satellite-based measurements of parameters. BC from wildfires increased markedly over the Northern Hemisphere in a warmer climate, enhancing BC deposition on the GrIS. Recent BC emissions in the Arctic were also attributed to shipping activities. The BC emissions from Arctic ship traffic have increased in recent years due to the decreased ice-sea extent, heightened last-chance tourism, and supply shipping to the offshore gas/oil extraction industries. During the most recent two decades, ice sheet melting for the last decade has been slowing down with the steady loss of GrIS. This result might be reflected in parallel with the trend of emissions from biomass burning and

ship traffic. However, observation (ground and satellite) model studies did show clear evidence of a relationship between ice melting rate and BC emissions. If the expected warming of Greenland is extended further to cause much larger wildfires in the future, this could indeed include substantial albedo changes with the accelerated melting of the GrIS. The study on the Arctic climate response to light-absorbing impurities should thus be explored further to properly project how this system interacts with the global climate system. Additionally, the predictions on the future GrIS mass loss should be made to help clarify the exact role of albedo change (due to light-absorbing impurities) in controlling the melting trend of GrIS.

Author Contributions: K.V.: Formal analysis; investigation; methodology; visualization; writing—review and editing; E.E.K.: Formal analysis; resources; software; validation; writing—review and editing; K.-H.K.: investigation; methodology; project administration; resources; software; supervision; validation; writing—review and editing; C.S.: Formal analysis; investigation; methodology; visualization; M.K.: Formal analysis; investigation; methodology; visualization; Z.-H.S.: Methodology; software; supervision; validation; writing—review and editing. All authors have read and agreed to the published version of the manuscript.

Funding: This research was supported by the Basic Science Research Program through the National Research Foundation of Korea (NRF) funded by the Ministry of Science, ICT and Future Planning (2018R1A2A1A05077650).

Conflicts of Interest: The authors declare no conflict of interest.

References

1. Aschwanden, A.; Fahnestock, M.A.; Truffer, M.; Brinkerhoff, D.J.; Hock, R.; Khroulev, C.; Mottram, R.; Khan, S.A. Contribution of the Greenland Ice Sheet to sea level over the next millennium. *Sci. Adv.* **2019**, *5*, eaav9396. [CrossRef]
2. Kintisch, E. The great Greenland meltdown. *Science* **2017**. [CrossRef]
3. IPCC. *Choices Made Now are Critical for the Future of Our Ocean and Cryosphere*; Intergovernmental Panel on Climate Change: Geneva, Switzerland, 2019.
4. Bottenheim, J.W.; Dastoor, A.; Gong, S.-L.; Higuchi, K.; Li, Y.-F. Long range transport of air pollution to the Arctic. In *Air Pollution: Intercontinental Transport of Air Pollution*; Stohl, A., Ed.; Springer: Berlin/Heidelberg, Germany, 2004; pp. 13–39. [CrossRef]
5. Coopman, Q.; Garrett, T.J.; Finch, D.P.; Riedi, J. High Sensitivity of Arctic Liquid Clouds to Long-Range Anthropogenic Aerosol Transport. *Geophys. Res. Lett.* **2018**, *45*, 372–381. [CrossRef]
6. Law, K.S.; Roiger, A.; Thomas, J.L.; Marelle, L.; Raut, J.-C.; Dalsøren, S.; Fuglestvedt, J.; Tuccella, P.; Weinzierl, B.; Schlager, H. Local Arctic air pollution: Sources and impacts. *Ambio* **2017**, *46*, 453–463. [CrossRef] [PubMed]
7. Coopman, Q.; Riedi, J.; Finch, D.P.; Garrett, T.J. Evidence for Changes in Arctic Cloud Phase Due to Long-Range Pollution Transport. *Geophys. Res. Lett.* **2018**, *45*, 10709–10718. [CrossRef]
8. Leahy, S. Greenland's ice is melting four times faster than thought—What it means. In *National Geographic*; National Geographic Society: Washington, DC, USA, 2019.
9. McComiskey, A.; Feingold, G.; Frisch, A.S.; Turner, D.D.; Miller, M.A.; Chiu, J.C.; Min, Q.; Ogren, J.A. An assessment of aerosol-cloud interactions in marine stratus clouds based on surface remote sensing. *J. Geophys. Res. Atmos.* **2009**, *114*. [CrossRef]
10. Garrett, T.J.; Brattström, S.; Sharma, S.; Worthy, D.E.J.; Novelli, P. The role of scavenging in the seasonal transport of black carbon and sulfate to the Arctic. *Geophys. Res. Lett.* **2011**, *38*. [CrossRef]
11. Bevis, M.; Harig, C.; Khan, S.A.; Brown, A.; Simons, F.J.; Willis, M.; Fettweis, X.; van den Broeke, M.R.; Madsen, F.B.; Kendrick, E.; et al. Accelerating changes in ice mass within Greenland, and the ice sheet's sensitivity to atmospheric forcing. *Proc. Natl. Acad. Sci. USA* **2019**, *116*, 1934. [CrossRef]
12. Kay, J.E.; L'Ecuyer, T. Observational constraints on Arctic Ocean clouds and radiative fluxes during the early 21st century. *J. Geophys. Res. Atmos.* **2013**, *118*, 7219–7236. [CrossRef]
13. Thomas, M.A.; Devasthale, A.; Tjernström, M.; Ekman, A.M.L. The Relation Between Aerosol Vertical Distribution and Temperature Inversions in the Arctic in Winter and Spring. *Geophys. Res. Lett.* **2019**, *46*, 2836–2845. [CrossRef]
14. Schmale, J.; Arnold, S.R.; Law, K.S.; Thorp, T.; Anenberg, S.; Simpson, W.R.; Mao, J.; Pratt, K.A. Local Arctic Air Pollution: A Neglected but Serious Problem. *Earth's Future* **2018**, *6*, 1385–1412. [CrossRef]
15. Zhao, C.; Garrett, T.J. Effects of Arctic haze on surface cloud radiative forcing. *Geophys. Res. Lett.* **2015**, *42*, 557–564. [CrossRef]
16. AMAP. *AMAP Climate Change Update 2019: An. Update to Key Findings of Snow, Water, Ice and Permafrost in the Arctic (SWIPA) 2017*; Arctic Monitoring and Assessment Programme (AMAP): Oslo, Norway, 2019.
17. Tedesco, M.; Doherty, S.; Fettweis, X.; Alexander, P.; Jeyaratnam, J.; Noble, E.; Stroeve, J.C. The darkening of the Greenland ice sheet: Trends, drivers, and projections (1981–2100). *Cryosphere Discuss.* **2016**, *9*, 5595–5645. [CrossRef]

18. Wiese, D.N.; Yuan, D.-N.; Boening, C.; Landerer, F.W.; Watkins, M.M. JPL GRACE Mascon Ocean, Ice, and Hydrology Equivalent Water Height RL05M.1 CRI Filtered Version 2. 2016. Available online: https://podaac.jpl.nasa.gov/dataset/TELLUS_GRACE_MASCON_CRI_GRID_RL05_V2 (accessed on 2 December 2020). [CrossRef]
19. Mouginot, J.; Rignot, E.; Bjørk, A.A.; van den Broeke, M.; Millan, R.; Morlighem, M.; Noël, B.; Scheuchl, B.; Wood, M. Forty-six years of Greenland Ice Sheet mass balance from 1972 to 2018. *Proc. Natl. Acad. Sci. USA* **2019**, *116*, 9239. [CrossRef] [PubMed]
20. Ahlstrøm, A.P.; Petersen, D.; Langen, P.L.; Citterio, M.; Box, J.E. Abrupt shift in the observed runoff from the southwestern Greenland ice sheet. *Sci. Adv.* **2017**, *3*, e1701169. [CrossRef]
21. Hanna, E.; Jones, J.M.; Cappelen, J.; Mernild, S.H.; Wood, L.; Steffen, K.; Huybrechts, P. The influence of North Atlantic atmospheric and oceanic forcing effects on 1900–2010 Greenland summer climate and ice melt/runoff. *Int. J. Climatol.* **2013**, *33*, 862–880. [CrossRef]
22. Lim, Y.-K.; Schubert, S.D.; Nowicki, S.M.J.; Lee, J.N.; Molod, A.M.; Cullather, R.I.; Zhao, B.; Velicogna, I. Atmospheric summer teleconnections and Greenland Ice Sheet surface mass variations: Insights from MERRA-2. *Environ. Res. Lett.* **2016**, *11*, 024002. [CrossRef]
23. McLeod, J.T.; Mote, T.L. Assessing the role of precursor cyclones on the formation of extreme Greenland blocking episodes and their impact on summer melting across the Greenland ice sheet. *J. Geophys. Res. Atmos.* **2015**, *120*, 12357–12377. [CrossRef]
24. Hurrell, J.W.; Kushnir, Y.; Ottersen, G.; Visbeck, M. An overview of the North Atlantic oscillation. In *The North Atlantic Oscillation: Climatic Significance and Environmental Impact*; American Geophysical Union: Washington, DC, USA, 2003; pp. 1–35. [CrossRef]
25. Hanna, E.; Hall, R.J.; Cropper, T.E.; Ballinger, T.J.; Wake, L.; Mote, T.; Cappelen, J. Greenland blocking index daily series 1851–2015: Analysis of changes in extremes and links with North Atlantic and UK climate variability and change. *Int. J. Climatol.* **2018**, *38*, 3546–3564. [CrossRef]
26. Chen, X.; Luo, D. Arctic sea ice decline and continental cold anomalies: Upstream and downstream effects of Greenland blocking. *Geophys. Res. Lett.* **2017**, *44*, 3411–3419. [CrossRef]
27. Hanna, E.; Cropper, T.E.; Hall, R.J.; Cappelen, J. Greenland Blocking Index 1851–2015: A regional climate change signal. *Int. J. Climatol.* **2016**, *36*, 4847–4861. [CrossRef]
28. Liu, C.; Barnes, E.A. Extreme moisture transport into the Arctic linked to Rossby wave breaking. *J. Geophys. Res. Atmos.* **2015**, *120*, 3774–3788. [CrossRef]
29. Woods, C.; Caballero, R.; Svensson, G. Large-scale circulation associated with moisture intrusions into the Arctic during winter. *Geophys. Res. Lett.* **2013**, *40*, 4717–4721. [CrossRef]
30. Zhu, Y.; Newell, R.E. A Proposed Algorithm for Moisture Fluxes from Atmospheric Rivers. *Mon. Weather Rev.* **1998**, *126*, 725–735. [CrossRef]
31. Mattingly, K.S.; Mote, T.L.; Fettweis, X. Atmospheric River Impacts on Greenland Ice Sheet Surface Mass Balance. *J. Geophys. Res. Atmos.* **2018**, *123*, 8538–8560. [CrossRef]
32. Doyle, S.H.; Hubbard, A.; van de Wal, R.S.W.; Box, J.E.; van As, D.; Scharrer, K.; Meierbachtol, T.W.; Smeets, P.C.J.P.; Harper, J.T.; Johansson, E.; et al. Amplified melt and flow of the Greenland ice sheet driven by late-summer cyclonic rainfall. *Nat. Geosci.* **2015**, *8*, 647–653. [CrossRef]
33. Binder, H.; Boettcher, M.; Grams, C.M.; Joos, H.; Pfahl, S.; Wernli, H. Exceptional Air Mass Transport and Dynamical Drivers of an Extreme Wintertime Arctic Warm Event. *Geophys. Res. Lett.* **2017**, *44*, 12028–12036. [CrossRef]
34. Hofer, S.; Tedstone, A.J.; Fettweis, X.; Bamber, J.L. Decreasing cloud cover drives the recent mass loss on the Greenland Ice Sheet. *Sci. Adv.* **2017**, *3*, e1700584. [CrossRef]
35. Fettweis, X.; Franco, B.; Tedesco, M.; van Angelen, J.H.; Lenaerts, J.T.M.; van den Broeke, M.R.; Gallée, H. Estimating the Greenland ice sheet surface mass balance contribution to future sea level rise using the regional atmospheric climate model MAR. *Cryosphere* **2013**, *7*, 469–489. [CrossRef]
36. Le clec'h, S.; Charbit, S.; Quiquet, A.; Fettweis, X.; Dumas, C.; Kageyama, M.; Wyard, C.; Ritz, C. Assessment of the Greenland ice sheet–atmosphere feedbacks for the next century with a regional atmospheric model coupled to an ice sheet model. *Cryosphere* **2019**, *13*, 373–395. [CrossRef]
37. Hirdman, D.; Burkhart, J.F.; Sodemann, H.; Eckhardt, S.; Jefferson, A.; Quinn, P.K.; Sharma, S.; Ström, J.; Stohl, A. Long-term trends of black carbon and sulphate aerosol in the Arctic: Changes in atmospheric transport and source region emissions. *Atmos. Chem. Phys.* **2010**, *10*, 9351–9368. [CrossRef]
38. Burkhart, J.F.; Bales, R.C.; McConnell, J.R.; Hutterli, M.A. Influence of North Atlantic Oscillation on anthropogenic transport recorded in northwest Greenland ice cores. *J. Geophys. Res. Atmos.* **2006**, *111*. [CrossRef]
39. Quinn, P.K.; Stohl, A.; Arneth, A.; Berntsen, T.; Burkhart, J.F.; Christensen, J.; Flanner, M.; Kupiainen, K.; Lihavainen, H.; Shepherd, M.; et al. *AMAP: The Impact of Black Carbon on Arctic Climate (2011)*; Arctic Monitoring and Assessment Programme (AMAP): Tromso, Norway, 2011.
40. AMAP. *Black Carbon and Ozone as Arctic Climate Forcers*; Arctic Monitoring and Assessment Programme (AMAP): Tromso, Norway, 2015.
41. Twomey, S. The Influence of Pollution on the Shortwave Albedo of Clouds. *J. Atmos. Sci.* **1977**, *34*, 1149–1152. [CrossRef]
42. McConnell, J.R.; Edwards, R.; Kok, G.L.; Flanner, M.G.; Zender, C.S.; Saltzman, E.S.; Banta, J.R.; Pasteris, D.R.; Carter, M.M.; Kahl, J.D.W. 20th-Century Industrial Black Carbon Emissions Altered Arctic Climate Forcing. *Science* **2007**, *317*, 1381. [CrossRef]

43. Bond, T.C.; Doherty, S.J.; Fahey, D.W.; Forster, P.M.; Berntsen, T.; DeAngelo, B.J.; Flanner, M.G.; Ghan, S.; Kärcher, B.; Koch, D.; et al. Bounding the role of black carbon in the climate system: A scientific assessment. *J. Geophys. Res. Atmos.* **2013**, *118*, 5380–5552. [CrossRef]
44. Flanner, M.G. Arctic climate sensitivity to local black carbon. *J. Geophys. Res. Atmos.* **2013**, *118*, 1840–1851. [CrossRef]
45. Church, J.; Clark, P.; Cazenave, A.; Gregory, J.; Jevrejeva, S.; Levermann, A.; Merrifield, M.; Milne, G.; Nerem, R.; Nunn, P.; et al. Climate Change 2013: The Physical Science Basis. Contribution of Working Group I to the Fifth Assessment Report of the Intergovernmental Panel on Climate Change. *Sea Level Chang.* **2013**, 1138–1191.
46. Mölders, N.; Edwin, S. Review of Black Carbon in the Arctic—Origin, Measurement Methods, and Observations. *Open J. Air Pollut.* **2018**, *7*, 181–213. [CrossRef]
47. Lutsch, E.M. *The Influence of Biomass Burning on the Arctic Atmosphere*; University of Toronto: Toronto, ON, Canada, 2019.
48. Comer, B.; Olmer, N.; Mao, X.; Roy, B.; Rutherford, D. *Prevalence of Heavy Fuel Oil and Black Carbon in Arctic Shipping, 2015 to 2025*; International Council on Clean Transportation: Washington, DC, USA, 2017.
49. Council, A.; Authors, C.; Brigham, L.; McCalla, R.; Cunningham, E.; Barr, W.; Vanderzaag, D.; Santos-Pedro, V.; MacDonald, R.; Harder, S.; et al. *Arctic Marine Shipping Assessment 2009 Report*; Protection of the Arctic Marine Environment: Akureyri, Iceland, 2009; p. 194.
50. Corbett, J.J.; Lack, D.A.; Winebrake, J.J.; Harder, S.; Silberman, J.A.; Gold, M. Arctic shipping emissions inventories and future scenarios. *Atmos. Chem. Phys.* **2010**, *10*, 9689–9704. [CrossRef]
51. Peters, G.P.; Nilssen, T.B.; Lindholt, L.; Eide, M.S.; Glomsrød, S.; Eide, L.I.; Fuglestvedt, J.S. Future emissions from shipping and petroleum activities in the Arctic. *Atmos. Chem. Phys.* **2011**, *11*, 5305–5320. [CrossRef]
52. Small, J.D.; Chuang, P.Y.; Feingold, G.; Jiang, H. Can aerosol decrease cloud lifetime? *Geophys. Res. Lett.* **2009**, *36*. [CrossRef]
53. Christensen, M.W.; Jones, W.K.; Stier, P. Aerosols enhance cloud lifetime and brightness along the stratus-to-cumulus transition. *Proc. Natl. Acad. Sci. USA* **2020**, *117*, 17591. [CrossRef] [PubMed]
54. Soja, A.J.; Tchebakova, N.M.; French, N.H.F.; Flannigan, M.D.; Shugart, H.H.; Stocks, B.J.; Sukhinin, A.I.; Parfenova, E.I.; Chapin, F.S.; Stackhouse, P.W. Climate-induced boreal forest change: Predictions versus current observations. *Glob. Planet. Chang.* **2007**, *56*, 274–296. [CrossRef]
55. Thomas, J.L.; Polashenski, C.M.; Soja, A.J.; Marelle, L.; Casey, K.A.; Choi, H.D.; Raut, J.C.; Wiedinmyer, C.; Emmons, L.K.; Fast, J.D.; et al. Quantifying black carbon deposition over the Greenland ice sheet from forest fires in Canada. *Geophys. Res. Lett.* **2017**, *44*, 7965–7974. [CrossRef]
56. Voulgarakis, A.; Field, R.D. Fire Influences on Atmospheric Composition, Air Quality and Climate. *Curr. Pollut. Rep.* **2015**, *1*, 70–81. [CrossRef]
57. Flanner, M.G.; Zender, C.S.; Randerson, J.T.; Rasch, P.J. Present-day climate forcing and response from black carbon in snow. *J. Geophys. Res. Atmos.* **2007**, *112*. [CrossRef]
58. Yttri, K.E.; Lund Myhre, C.; Eckhardt, S.; Fiebig, M.; Dye, C.; Hirdman, D.; Strom, J.; Klimont, Z.; Stohl, A. Quantifying black carbon from biomass burning by means of levoglucosan-a one-year time series at the Arctic observatory Zeppelin. *Atmos. Chem. Phys.* **2014**, *14*, 6427–6442. [CrossRef]
59. Sharma, S.; Andrews, E.; Barrie, L.A.; Ogren, J.A.; Lavoué, D. Variations and sources of the equivalent black carbon in the high Arctic revealed by long-term observations at Alert and Barrow: 1989–2003. *J. Geophys. Res. Atmos.* **2006**, *111*. [CrossRef]
60. Sharma, S.; Ishizawa, M.; Chan, D.; Lavoué, D.; Andrews, E.; Eleftheriadis, K.; Maksyutov, S. 16-year simulation of Arctic black carbon: Transport, source contribution, and sensitivity analysis on deposition. *J. Geophys. Res. Atmos.* **2013**, *118*, 943–964. [CrossRef]
61. Stone, R.; Sharma, S.; Herber, A.; Eleftheriadis, K.; Nelson, D. A characterization of Arctic aerosols on the basis of aerosol optical depth and black carbon measurements. *Elem. Sci. Anthr.* **2014**, *2*. [CrossRef]
62. Vestreng, V.; Kallenborn, R.; Økstad, E. *Climate Influencing Emissions, Scenarios and Mitigation Options at Svalbard*; Norwegian Environment Agency: Oslo, Norway, 2010.
63. Kaufman, Y.J.; Ichoku, C.; Giglio, L.; Korontzi, S.; Chu, D.A.; Hao, W.M.; Li, R.R.; Justice, C.O. Fire and smoke observed from the Earth Observing System MODIS instrument–products, validation, and operational use. *Int. J. Remote Sens.* **2003**, *24*, 1765–1781. [CrossRef]
64. Di Giuseppe, F.; Pappenberger, F.; Wetterhall, F.; Krzeminski, B.; Camia, A.; Libertá, G.; San Miguel, J. The Potential Predictability of Fire Danger Provided by Numerical Weather Prediction. *J. Appl. Meteorol. Climatol.* **2016**, *55*, 2469–2491. [CrossRef]
65. Kaiser, J.W.; Heil, A.; Andreae, M.O.; Benedetti, A.; Chubarova, N.; Jones, L.; Morcrette, J.J.; Razinger, M.; Schultz, M.G.; Suttie, M.; et al. Biomass burning emissions estimated with a global fire assimilation system based on observed fire radiative power. *Biogeosciences* **2012**, *9*, 527–554. [CrossRef]
66. Evangeliou, N.; Kylling, A.; Eckhardt, S.; Myroniuk, V.; Stebel, K.; Paugam, R.; Zibtsev, S.; Stohl, A. Open fires in Greenland in summer 2017: Transport, deposition and radiative effects of BC, OC and BrC emissions. *Atmos. Chem. Phys.* **2019**, *19*, 1393–1411. [CrossRef]
67. Doerr, S.H.; Santín, C. Global trends in wildfire and its impacts: Perceptions versus realities in a changing world. *Philos. Trans. R. Soc. B Biol. Sci.* **2016**, *371*, 20150345. [CrossRef] [PubMed]
68. Giglio, L.; Randerson, J.T.; van der Werf, G.R. Analysis of daily, monthly, and annual burned area using the fourth-generation global fire emissions database (GFED4). *J. Geophys. Res. Biogeosciences* **2013**, *118*, 317–328. [CrossRef]

69. Ward, D.S.; Shevliakova, E.; Malyshev, S.; Lamarque, J.F.; Wittenberg, A.T. Variability of fire emissions on interannual to multi-decadal timescales in two Earth System models. *Environ. Res. Lett.* **2016**, *11*, 125008. [CrossRef]
70. Riihelä, A.; King, M.D.; Anttila, K. The surface albedo of the Greenland Ice Sheet between 1982 and 2015 from the CLARA-A2 dataset and its relationship to the ice sheet's surface mass balance. *Cryosphere* **2019**, *13*, 2597–2614. [CrossRef]
71. Yallop, M.L.; Anesio, A.M.; Perkins, R.G.; Cook, J.; Telling, J.; Fagan, D.; MacFarlane, J.; Stibal, M.; Barker, G.; Bellas, C.; et al. Photophysiology and albedo-changing potential of the ice algal community on the surface of the Greenland ice sheet. *ISME J.* **2012**, *6*, 2302–2313. [CrossRef]
72. Wiscombe, W.J.; Warren, S.G. A Model for the Spectral Albedo of Snow. I: Pure Snow. *J. Atmos. Sci.* **1980**, *37*, 2712–2733. [CrossRef]
73. Lutz, S.; Anesio, A.M.; Jorge Villar, S.E.; Benning, L.G. Variations of algal communities cause darkening of a Greenland glacier. *FEMS Microbiol. Ecol.* **2014**, *89*, 402–414. [CrossRef] [PubMed]
74. Van den Broeke, M.R.; Enderlin, E.M.; Howat, I.M.; Kuipers Munneke, P.; Noël, B.P.Y.; van de Berg, W.J.; van Meijgaard, E.; Wouters, B. On the recent contribution of the Greenland ice sheet to sea level change. *Cryosphere* **2016**, *10*, 1933–1946. [CrossRef]
75. Enderlin, E.M.; Howat, I.M.; Jeong, S.; Noh, M.-J.; van Angelen, J.H.; van den Broeke, M.R. An improved mass budget for the Greenland ice sheet. *Geophys. Res. Lett.* **2014**, *41*, 866–872. [CrossRef]
76. Dumont, M.; Brun, E.; Picard, G.; Michou, M.; Libois, Q.; Petit, J.R.; Geyer, M.; Morin, S.; Josse, B. Contribution of light-absorbing impurities in snow to Greenland's darkening since 2009. *Nat. Geosci.* **2014**, *7*, 509–512. [CrossRef]
77. Keegan, K.M.; Albert, M.R.; McConnell, J.R.; Baker, I. Climate change and forest fires synergistically drive widespread melt events of the Greenland Ice Sheet. *Proc. Natl. Acad. Sci. USA* **2014**, *111*, 7964. [CrossRef] [PubMed]
78. Polashenski, C.M.; Dibb, J.E.; Flanner, M.G.; Chen, J.Y.; Courville, Z.R.; Lai, A.M.; Schauer, J.J.; Shafer, M.M.; Bergin, M. Neither dust nor black carbon causing apparent albedo decline in Greenland's dry snow zone: Implications for MODIS C5 surface reflectance. *Geophys. Res. Lett.* **2015**, *42*, 9319–9327. [CrossRef]
79. Tedstone, A.J.; Cook, J.M.; Williamson, C.J.; Hofer, S.; McCutcheon, J.; Irvine-Fynn, T.; Gribbin, T.; Tranter, M. Algal growth and weathering crust state drive variability in western Greenland Ice Sheet ice albedo. *Cryosphere* **2020**, *14*, 521–538. [CrossRef]
80. Stohl, A.; Andrews, E.; Burkhart, J.F.; Forster, C.; Herber, A.; Hoch, S.W.; Kowal, D.; Lunder, C.; Mefford, T.; Ogren, J.A.; et al. Pan-Arctic enhancements of light absorbing aerosol concentrations due to North American boreal forest fires during summer 2004. *J. Geophys. Res. Atmos.* **2006**, *111*. [CrossRef]
81. Schmeisser, L.; Backman, J.; Ogren, J.A.; Andrews, E.; Asmi, E.; Starkweather, S.; Uttal, T.; Fiebig, M.; Sharma, S.; Eleftheriadis, K.; et al. Seasonality of aerosol optical properties in the Arctic. *Atmos. Chem. Phys.* **2018**, *18*, 11599–11622. [CrossRef]
82. SESS. *Atmospheric Black Carbon in Svalbard (ABC Svalbard)—The State of Environmental Science in Svalbard (SESS) Report*; Svalbard Integrated Arctic Earth Obeserving System: Longyearbyen, Norway, 2019.
83. Sharma, S.; Lavoué, D.; Cachier, H.; Barrie, L.A.; Gong, S.L. Long-term trends of the black carbon concentrations in the Canadian Arctic. *J. Geophys. Res. Atmos.* **2004**, *109*. [CrossRef]
84. Shen, Z.; Ming, Y.; Horowitz, L.W.; Ramaswamy, V.; Lin, M. On the Seasonality of Arctic Black Carbon. *J. Clim.* **2017**, *30*, 4429–4441. [CrossRef]
85. Collaud Coen, M.; Andrews, E.; Alastuey, A.; Arsov, T.P.; Backman, J.; Brem, B.T.; Bukowiecki, N.; Couret, C.; Eleftheriadis, K.; Flentje, H.; et al. Multidecadal trend analysis of aerosol radiative properties at a global scale. *Atmos. Chem. Phys.* **2020**, *2020*, 1–54. [CrossRef]
86. Hansen, J.; Nazarenko, L. Soot climate forcing via snow and ice albedos. *Proc. Natl. Acad. Sci. USA* **2004**, *101*, 423. [CrossRef] [PubMed]
87. Jacobson, M.Z. Climate response of fossil fuel and biofuel soot, accounting for soot's feedback to snow and sea ice albedo and emissivity. *J. Geophys. Res. Atmos.* **2004**, *109*. [CrossRef]
88. Jacobson, M.Z. Short-term effects of controlling fossil-fuel soot, biofuel soot and gases, and methane on climate, Arctic ice, and air pollution health. *J. Geophys. Res. Atmos.* **2010**, *115*. [CrossRef]
89. Koch, D.; Menon, S.; Del Genio, A.; Ruedy, R.; Alienov, I.; Schmidt, G.A. Distinguishing Aerosol Impacts on Climate over the Past Century. *J. Clim.* **2009**, *22*, 2659–2677. [CrossRef]
90. Shindell, D.; Kuylenstierna, J.C.I.; Vignati, E.; van Dingenen, R.; Amann, M.; Klimont, Z.; Anenberg, S.C.; Muller, N.; Janssens-Maenhout, G.; Raes, F.; et al. Simultaneously Mitigating Near-Term Climate Change and Improving Human Health and Food Security. *Science* **2012**, *335*, 183. [CrossRef]
91. Hansen, J.; Sato, M.; Ruedy, R.; Nazarenko, L.; Lacis, A.; Schmidt, G.A.; Russell, G.; Aleinov, I.; Bauer, M.; Bauer, S.; et al. Efficacy of climate forcings. *J. Geophys. Res. Atmos.* **2005**, *110*. [CrossRef]
92. Shindell, D.; Faluvegi, G. Climate response to regional radiative forcing during the twentieth century. *Nat. Geosci.* **2009**, *2*, 294–300. [CrossRef]
93. Williamson, C.J.; Cook, J.; Tedstone, A.; Yallop, M.; McCutcheon, J.; Poniecka, E.; Campbell, D.; Irvine-Fynn, T.; McQuaid, J.; Tranter, M.; et al. Algal photophysiology drives darkening and melt of the Greenland Ice Sheet. *Proc. Natl. Acad. Sci. USA* **2020**, *117*, 5694. [CrossRef]
94. Ryan, J.C.; Hubbard, A.; Stibal, M.; Irvine-Fynn, T.D.; Cook, J.; Smith, L.C.; Cameron, K.; Box, J. Dark zone of the Greenland Ice Sheet controlled by distributed biologically-active impurities. *Nat. Commun.* **2018**, *9*, 1065. [CrossRef] [PubMed]
95. Nicholes, M.J.; Williamson, C.J.; Tranter, M.; Holland, A.; Poniecka, E.; Yallop, M.L.; Black; Bloom, G.; Anesio, A. Bacterial Dynamics in Supraglacial Habitats of the Greenland Ice Sheet. *Front. Microbiol.* **2019**, *10*, 1366. [CrossRef] [PubMed]

96. Lenton, T.M.; Rockstrom, J.; Gaffney, O.; Rahmstorf, S.; Richardson, K.; Steffen, W.; Schellnhuber, H.J. Climate tipping points—Too risky to bet against. *Nature* **2019**, *575*, 592–595. [CrossRef] [PubMed]
97. Pérez Ortega, R. Unusual Arctic Warming Explained by Overlooked Greenhouse Gases. Science. 2020. Available online: https://www.sciencemag.org/news/2020/01/unusual-arctic-warming-explained-overlooked-greenhouse-gases#:~{}:text=Unusual%20Arctic%20warming%20explained%20by%20overlooked%20greenhouse%20gases,-By%20Rodrigo%20P%C3%A9rez&text=Scientists%20looked%20at%20the%20effect,during%20that%20period%2C%20Nature%20reports. (accessed on 2 December 2020).